

Solar cycle modulation of galactic cosmic rays using a generalized force-field approximation

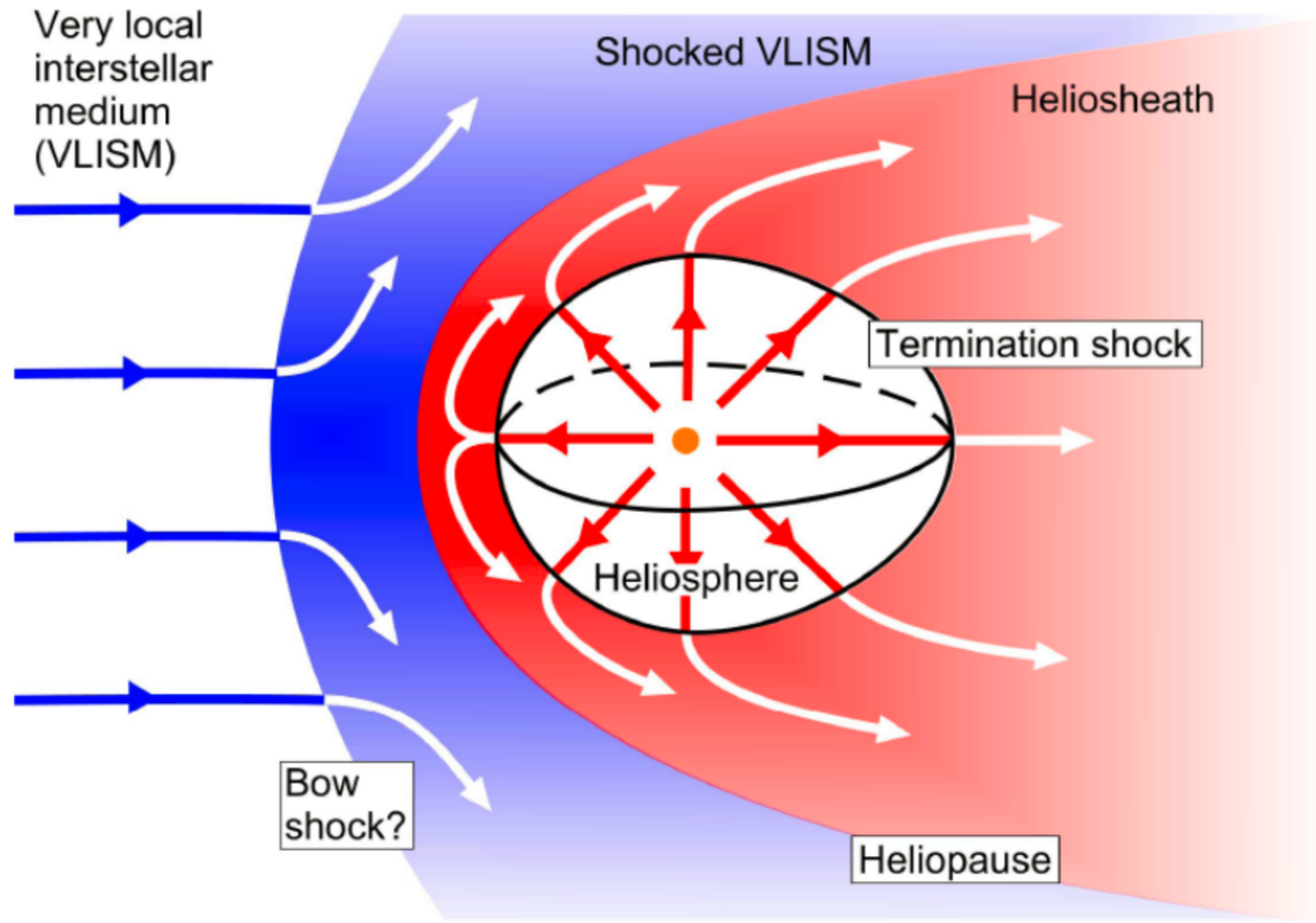
Zhen-Ning Shen (申振宁), Gang Li (李刚)

State Key Laboratory of Lunar and Planetary Sciences,
Macau University of Science and Technology

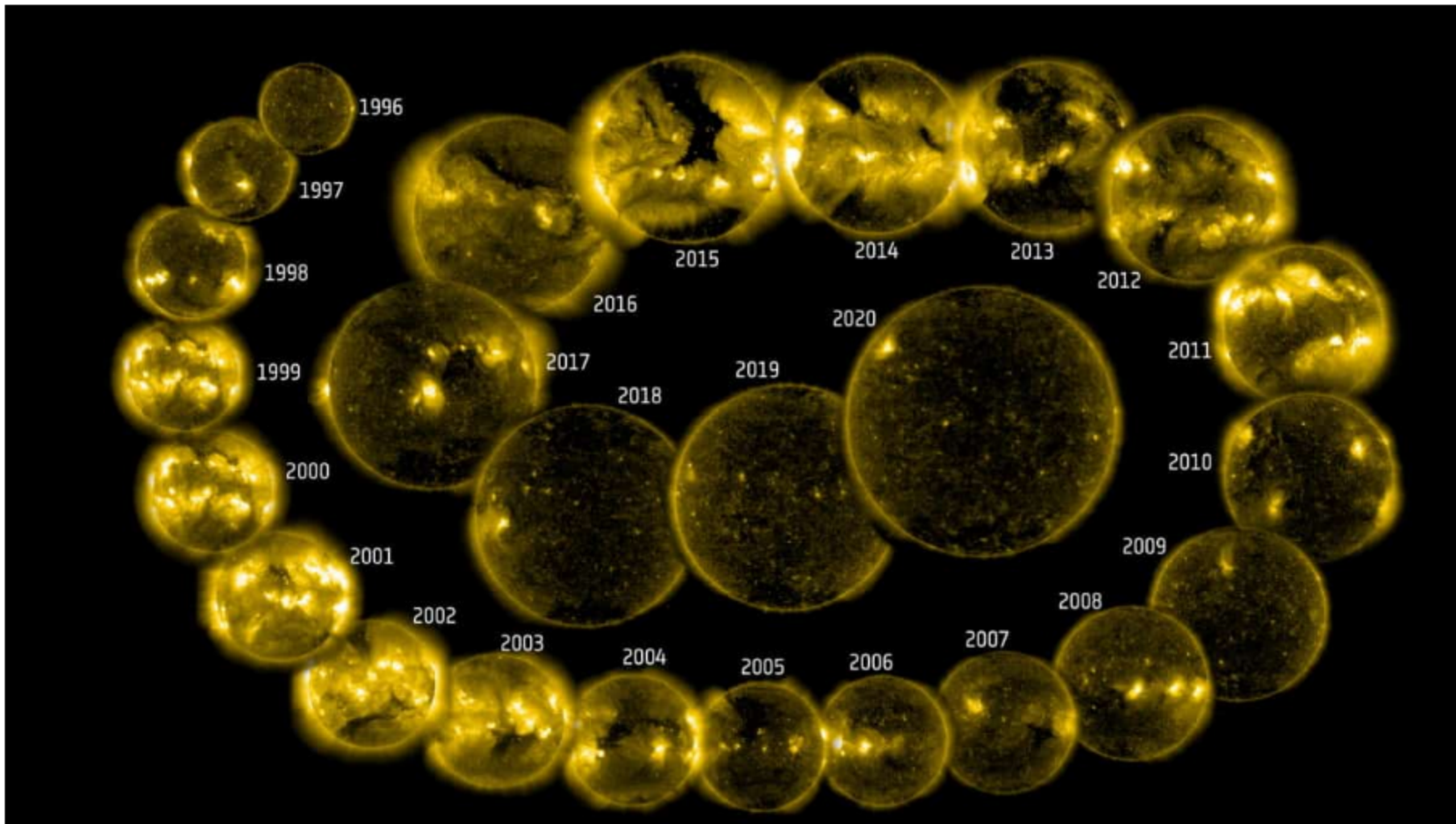
Outline

- **Introduction**
- **The Generalized Force-field Approximation**
- **Result**
- **Discussion**
- **Conclusion**

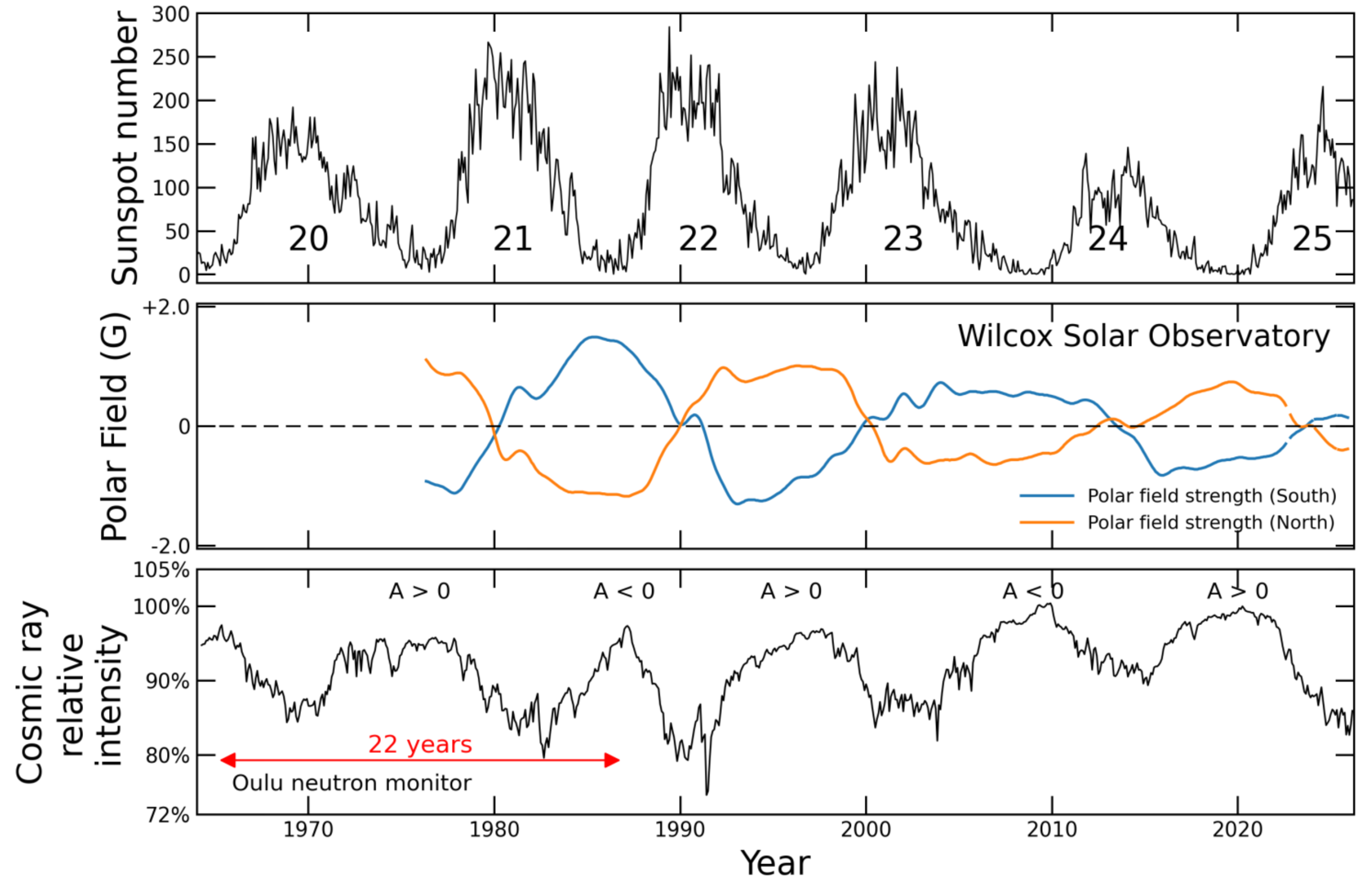
Introduction



日球层结构示意图(Owens and Forsyth 2013)



SOHO EIT观测的太阳图像(源自physicsworld网站)



Introduction

$$\frac{\partial U}{\partial t} = \nabla \cdot \left(\underbrace{\mathbf{K}^S \cdot \nabla U}_{\text{Diffusion}} - \underbrace{\mathbf{V}_{\text{sw}} U}_{\text{Convection}} - \underbrace{\langle \mathbf{v}_D \rangle U}_{\text{Drift}} \right) + \underbrace{\frac{1}{3} (\nabla \cdot \mathbf{V}_{\text{sw}}) \frac{\partial}{\partial T} (\alpha T U)}_{\text{Energetic Loss}}$$

Parker
transport
equation:

Diffusion
Small Scale
magnetic Field
irregularity

Convection
Solar wind
moving out
from the Sun

Drift
Large scale
magnetic field
structure

Energetic Loss
Due to adiabatic
expansion of the
solar wind

Numerical models (H-Ni):

- Empirical diffusion/drift coefficient model:
free parameter --> solar activity
 - Finite difference method:
 - ✓ 1D Badhwar-O' Neill model, (Slaba & Whitman 2020)
 - Stochastic differential equation method:
 - ✓ 2D HelMod model (Boschini et al. 2018)
 - ✓ 3D SDEMMA (Song et al. 2021)
- Ab-initio model (Shen et al. 2018, 2019)

Empirical or semiempirical models (H-Ni):

- modulation parameter --> solar activity
- ISO 15930 model (ISO 2004)
 - DLR (Matthia et al. 2013)
 - SINP (Kuznetsov et al. 2017)
 - CREME (Adams et al. 2012)
- Modified Force-field Approach (Shen et al. 2021, 2025)

Introduction

The Force-Field Solution (Gleeson & Axford 1968):

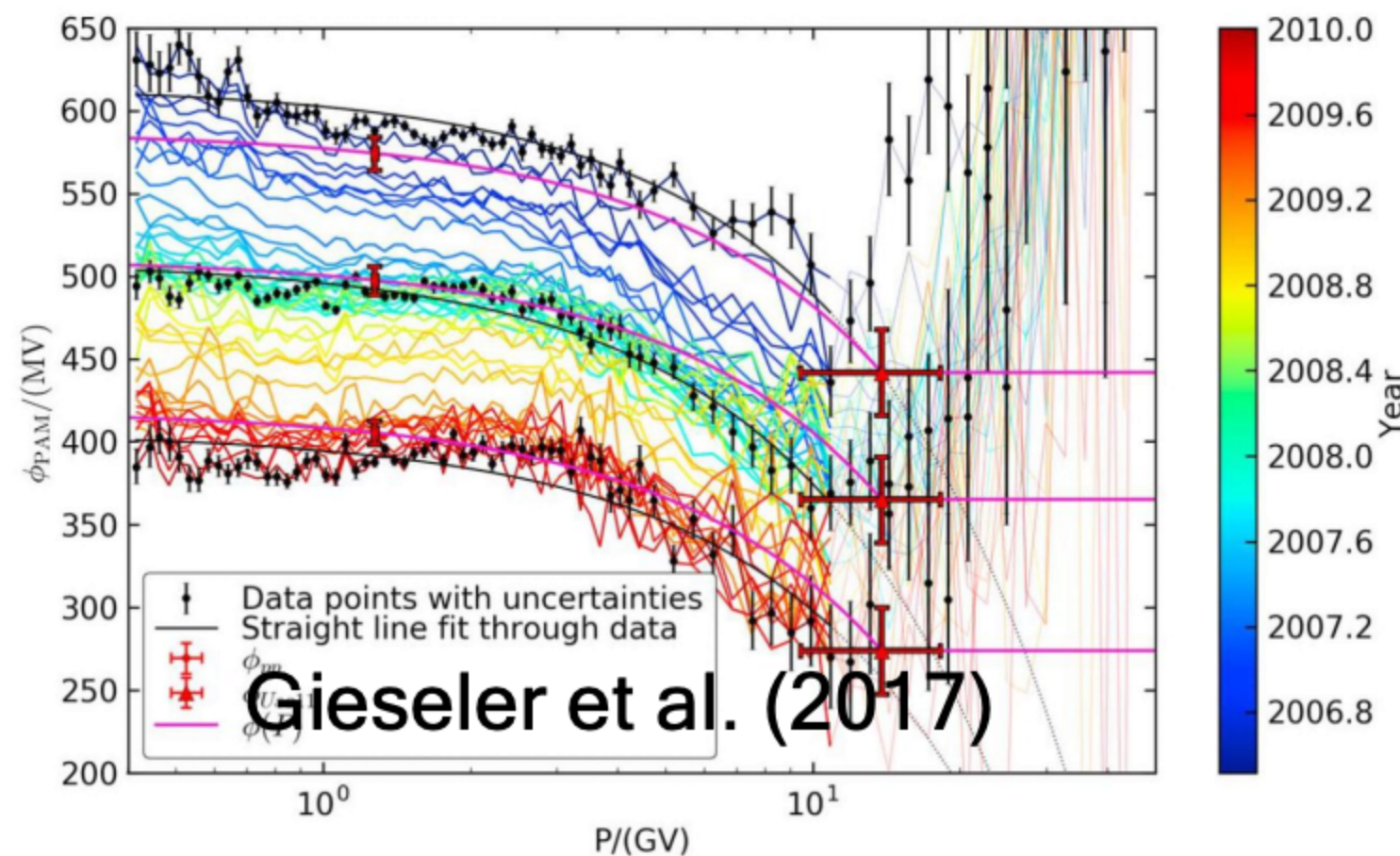
$$\frac{\partial f}{\partial r} + \frac{VP}{3\kappa} \frac{\partial f}{\partial P} = 0, \quad \kappa(r, P) = \beta \kappa_1(r) \kappa_2(P)$$

$$\frac{A}{Z} \int_E^{E_b} \frac{\kappa_2(P')}{P'} dE' = \int_r^{r_b} \frac{V(r')}{3\kappa(r')} dr' \equiv \phi(r)$$

ϕ is the Force-Field parameter.

If set $\kappa_2(P) = P$, we can get $E_b = E + \Phi$

$\Phi = \frac{Ze}{A} \phi$, constant for GCRs across all energies.



linear rigidity
dependence is
not accurate.

Corti et al. (2016)
$$\phi(R) = \begin{cases} \phi_L, & R < R_L \\ f(R, \phi_L, \phi_H), & R_L \leq R \leq R_H \\ \phi_H, & R > R_H, \end{cases}$$

Gieseler et al. (2017)
$$\phi(P) = \begin{cases} \frac{\phi_{Uso11} - \phi_{pp}}{P_{Uso11} - P_{pp}} \cdot (P - P_{pp}) + \phi_{pp} & \text{if } P < P_{Uso11} \\ \phi_{Uso11} & \text{if } P \geq P_{Uso11} \end{cases}$$

Zhu et al. (2024)
$$\phi(R) = \phi_l + \left(\frac{\phi_h - \phi_l}{1 + e^{(-R+R_b)}} \right)$$

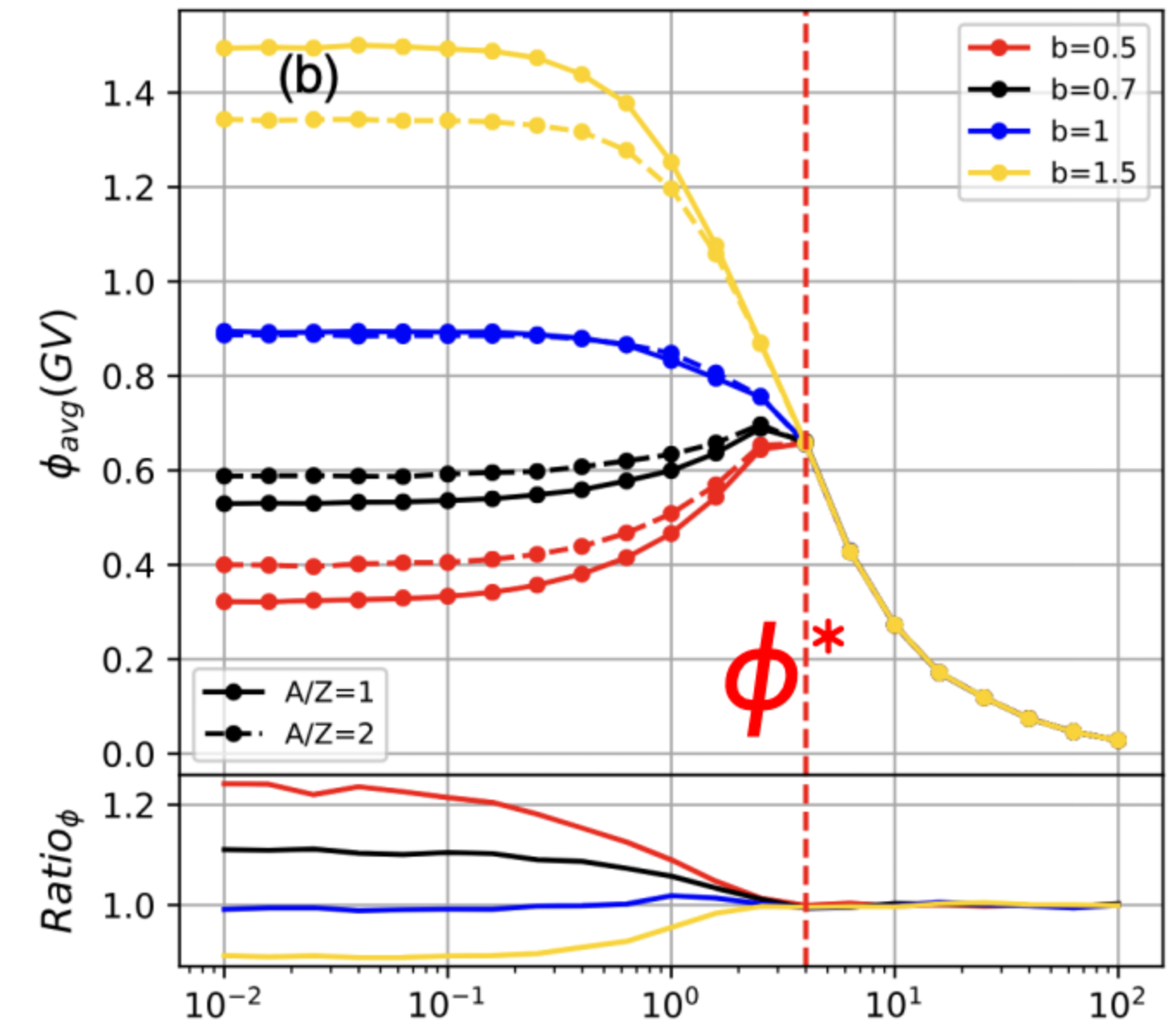
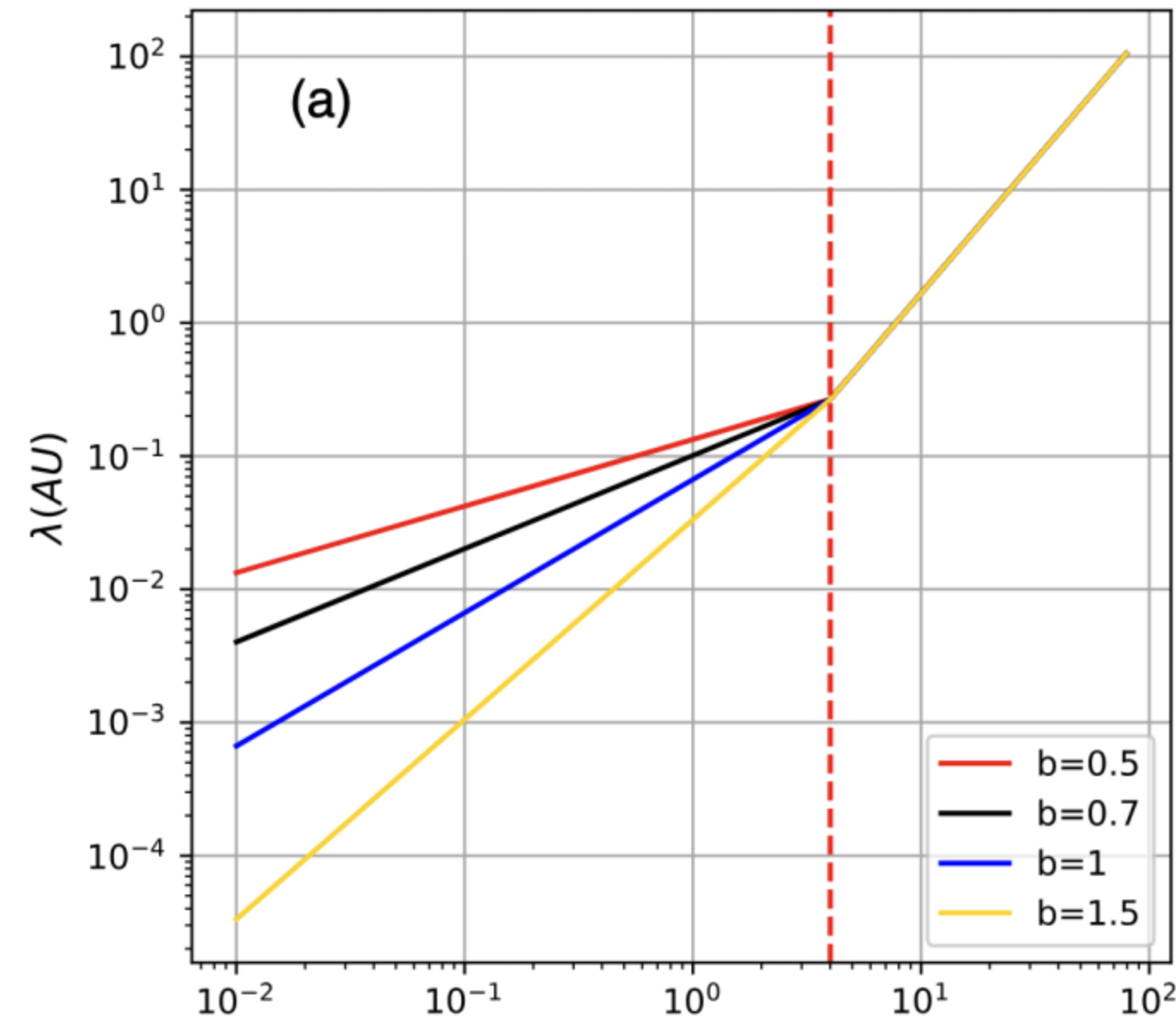
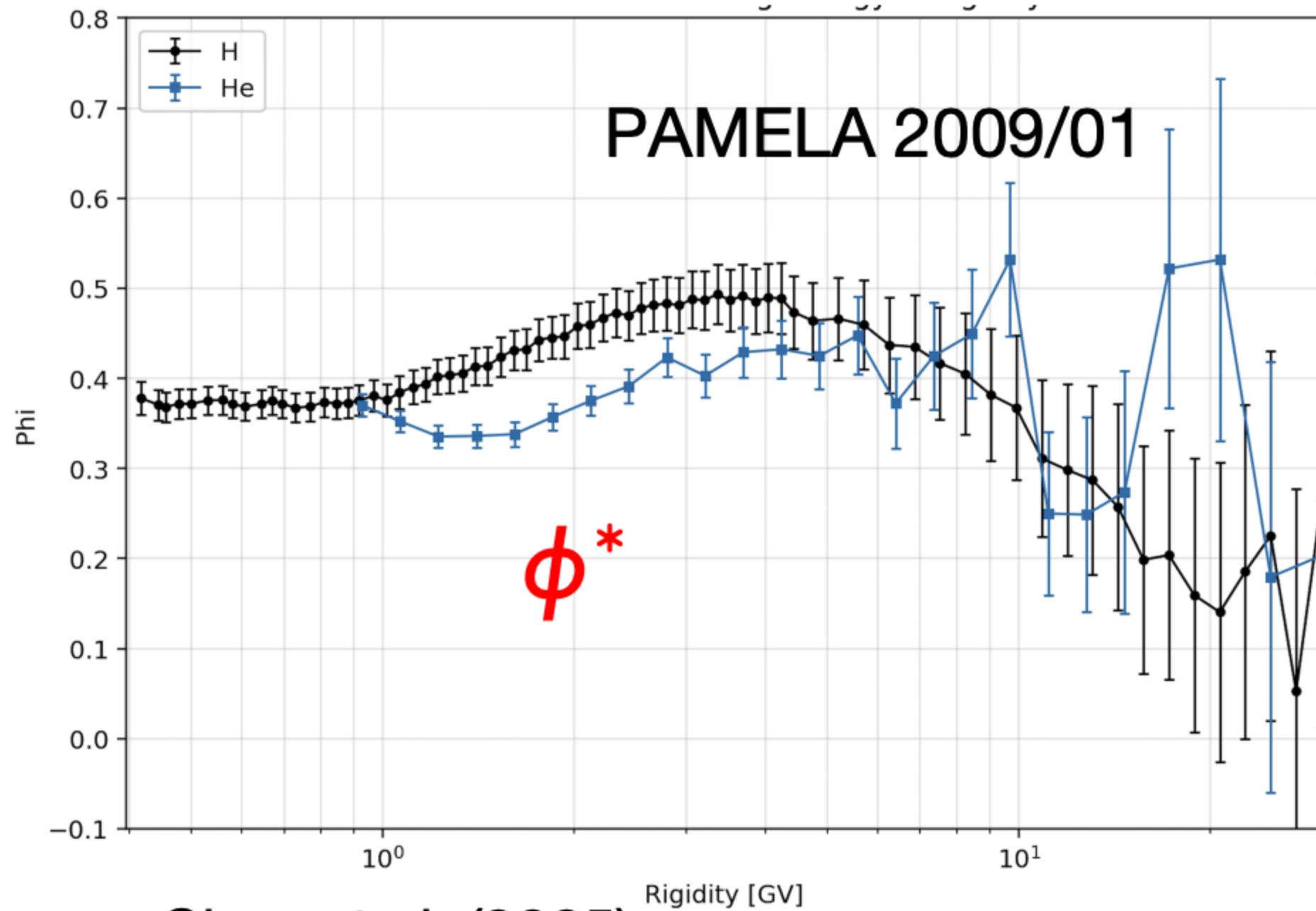
Shen et al. (2025)
$$\phi = \phi_0 \left[1 + \left(\frac{E}{E_{b1}} \right)^{\phi_1} \right]^{s_1} \exp \left[- \left(\frac{E}{E_{b2}} \right)^{s_2} \right]$$

➤ Effective modulation potential ϕ^* , satisfy

$$E_b = E + \frac{Z}{A} \phi^*$$

➤ The physical interpretation of the time and rigidity-dependent parameters remains unclear.

Introduction



Song et al. (2021)

Shen et al. (2025): A/Z dependence is required to reproduce low energy (<2 GV) spectra.

Song et al. (2021): Significant A/Z dependence below ~ 4 GV when the diffusion coefficient is no longer assumed to have a linear dependence on rigidity.

$$\phi = \frac{A}{Z} \int_E^{E_b} \frac{\kappa_2(P')}{P'} dE'$$

$$K_{\parallel} = K_0 \beta k_1(r) k_2(R),$$

$$k_1 = B_{eq}/B,$$

$$k_2 = \begin{cases} (R/R_k)^b & R < R_k \\ (R/R_k)^c & R \geq R_k \end{cases}$$

- The specific form of $\kappa_2(P')$?
- Can this explain the A/Z modulation effect?

Outline

- Introduction
- **The Generalized Force-field Approximation**
- Result
- Discussion
- Conclusion

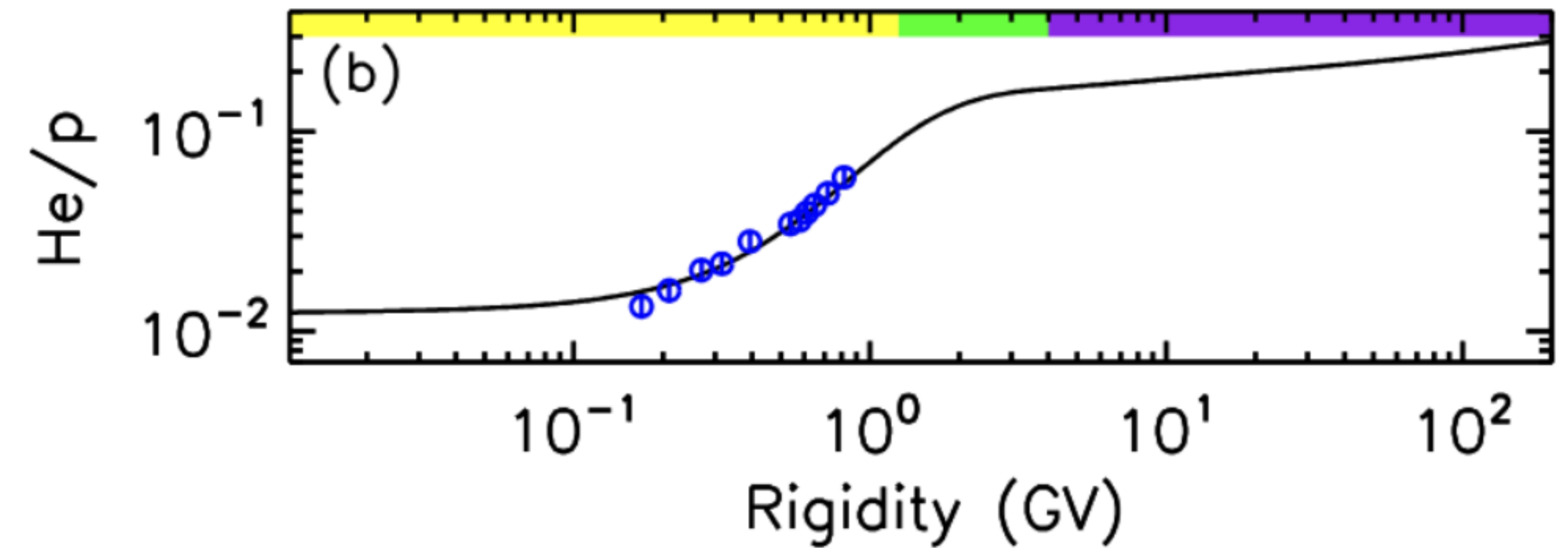
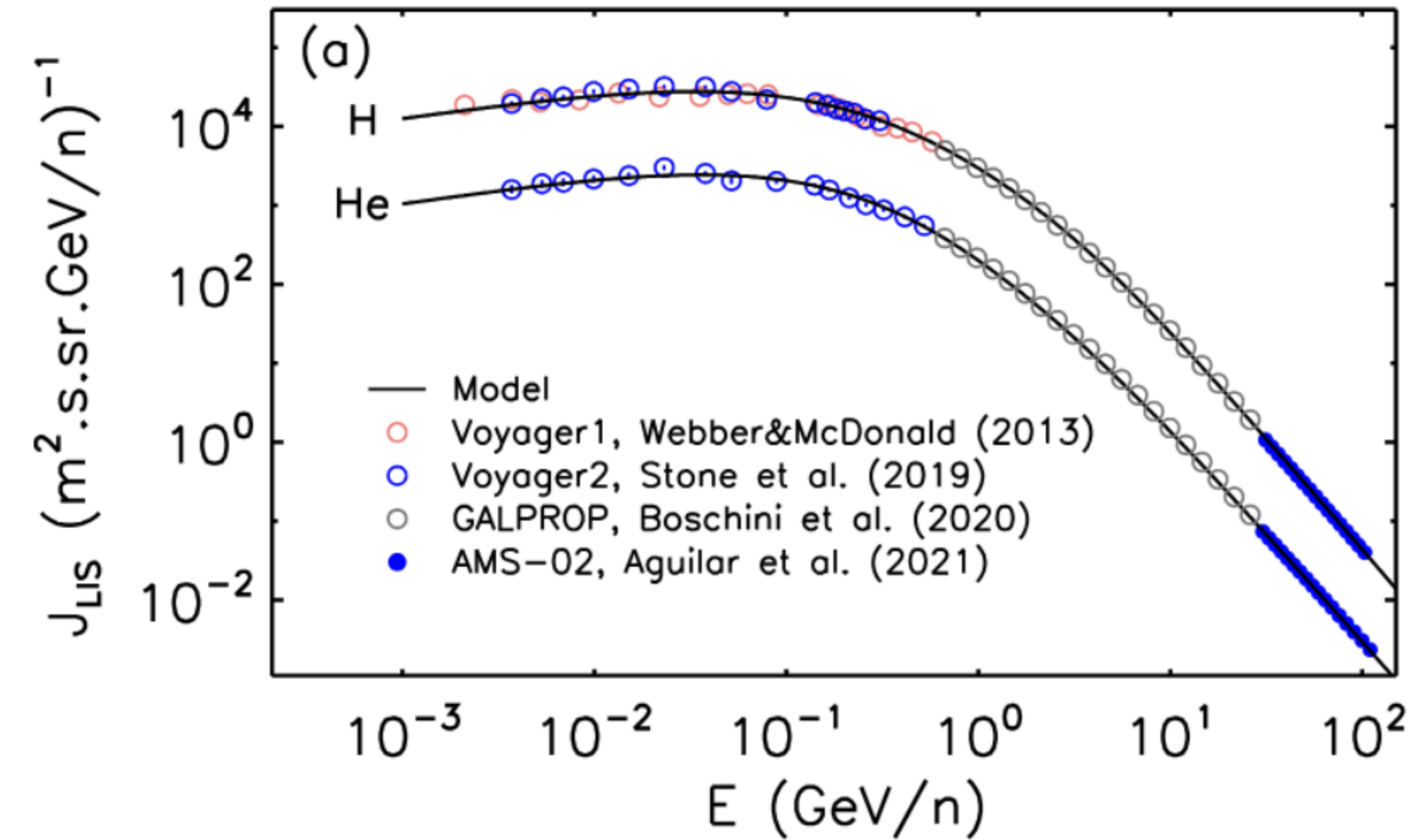
A generalized force-field approximation

$$\phi = \frac{A}{Z} \int_E^{E_b} \frac{K_2(P)}{P} dE'$$
$$J(E) = J_{LIS}(E_b) \frac{E(E + 2E_0)}{E_b(E_b + 2E_0)}$$

$$\text{LIS: } j_{LIS}(E) = a_0 \left(\frac{E}{E_b}\right)^{a_1} \left[1 + \left(\frac{E}{a_2}\right)^{a_3}\right]^{a_4} \left[1 + \left(\frac{E}{a_5}\right)^{a_6}\right]^{a_7}$$

Proton

- Voyager 1 and 2, beyond the heliopause (<0.6 GeV/n)
- 30 – 100 GeV/n at 1 AU , solar modulation become negligible
- 0.6 – 30 GeV/n, GALPROP model



A generalized force-field approximation

The generalized force field approximation:

$$J(E) = J_{\text{LIS}}(E_b) \frac{E(E + 2E_0)}{E_b(E_b + 2E_0)}$$

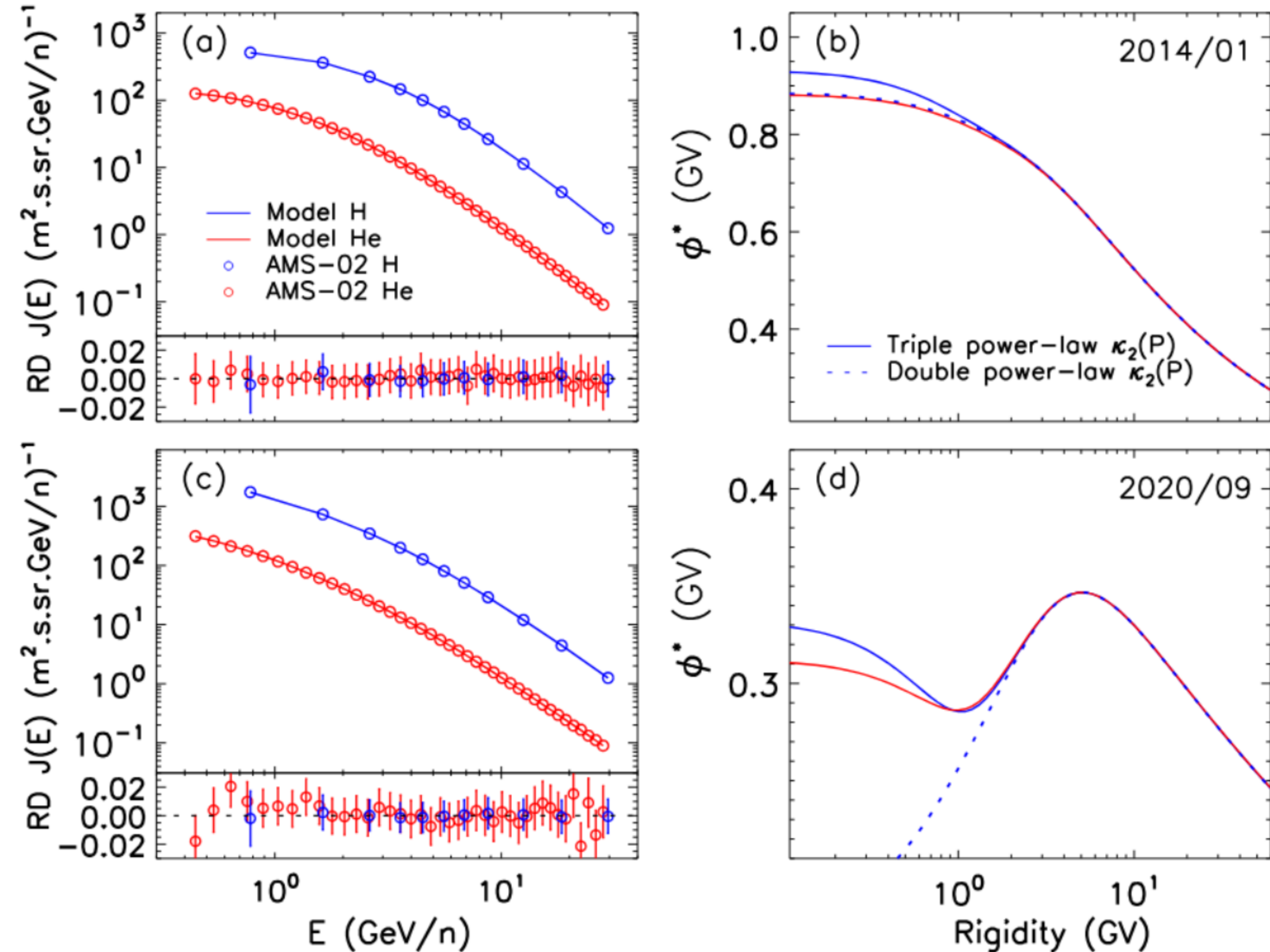
$$\phi = \frac{A}{Z} \int_E^{E_b} \frac{\kappa_2(P)}{P} dE'$$

$$\kappa_2(P) = P_0 \left(\frac{P}{P_0} \right)^{\gamma_0} \left(1 + \left(\frac{P}{P_{k1}} \right)^{s_1} \right)^{\frac{\gamma_1 - \gamma_0}{s_1}} \left(1 + \left(\frac{P}{P_{k2}} \right)^{s_2} \right)^{\frac{\gamma_2 - \gamma_1}{s_2}}$$

- $P_0 = 1\text{GV}$, $P_{k2} = 4.0\text{GV}$, $s_2 = 2.5$. At high rigidities, employ values used in numerical models.
- $\gamma_0 = 1.25$, $P_{k1} = 1.25\text{GV}$, $s_1 = 5.0$, by fitting to PAMELA (Martucci et al. 2018) and AMS-02 data (Aguilar et al. 2025).

Time dependent parameters: ϕ , γ_1 , γ_2

$$\phi^* = \frac{A}{Z} (E_b - E)$$

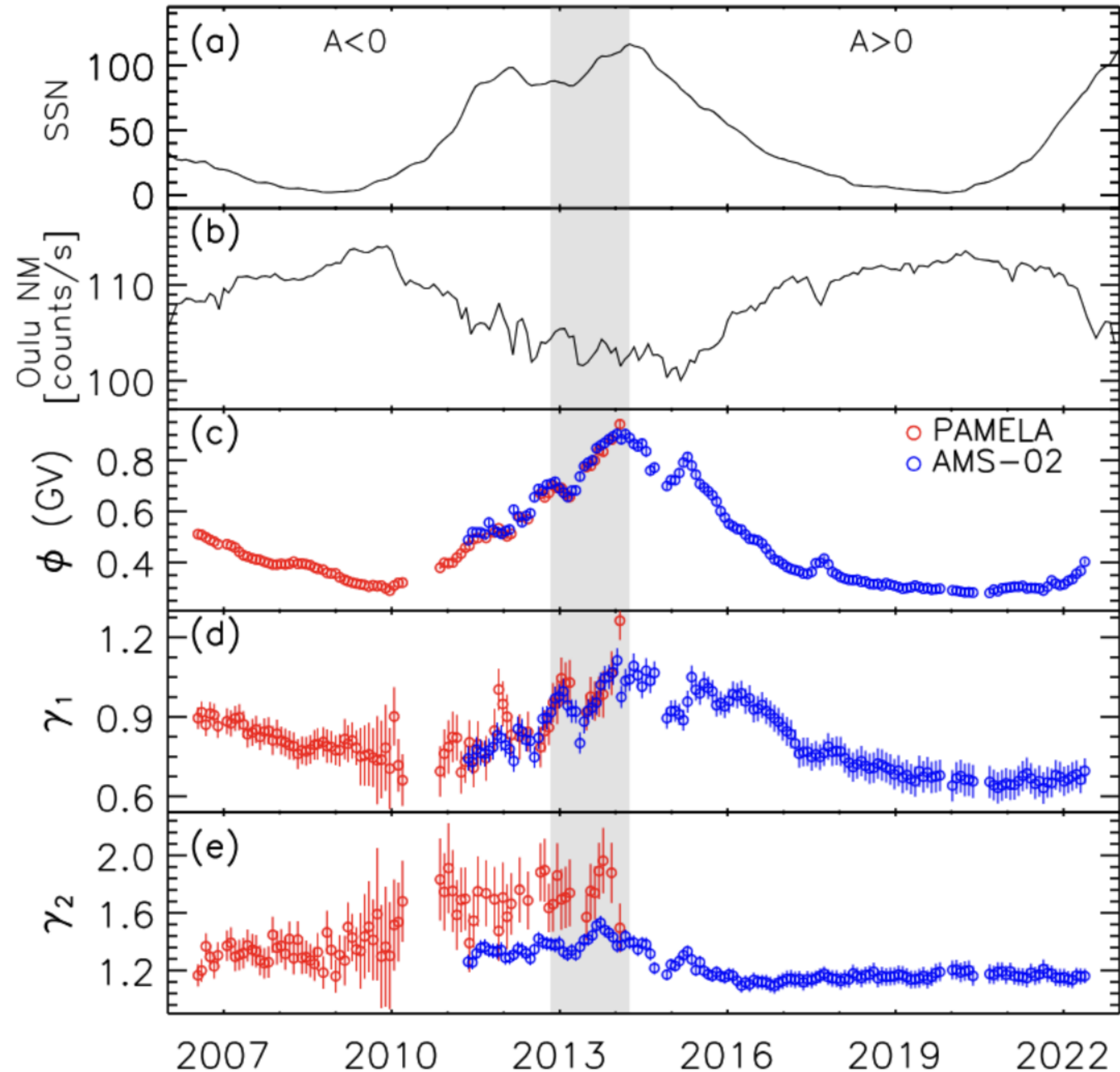


$\kappa_2(P)$: trajectory-integrated measure of particle transport from the modulation boundary to the observer.

Outline

- Introduction
- The Generalized Force-field Approximation
- Result
- Discussion
- Conclusion

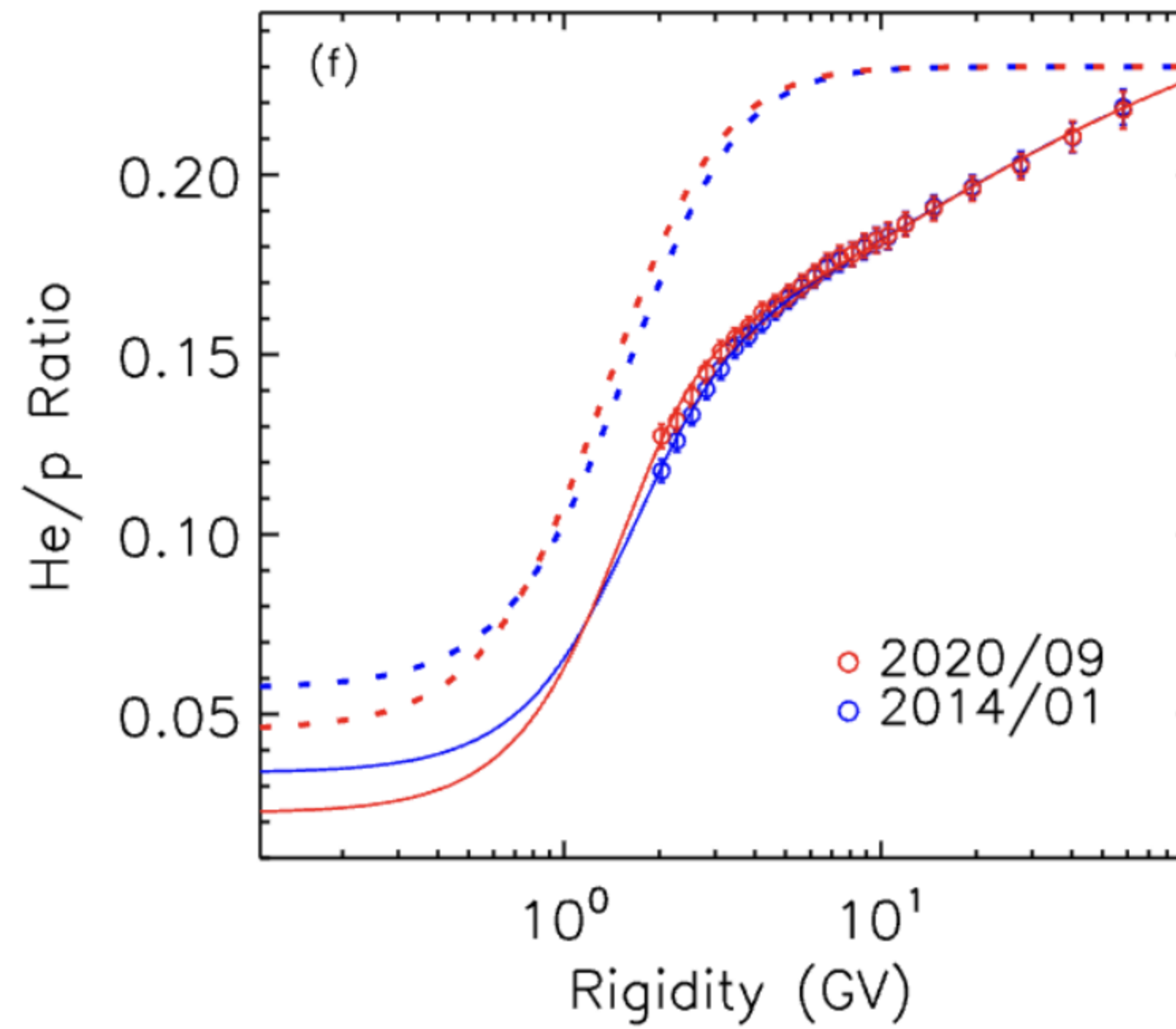
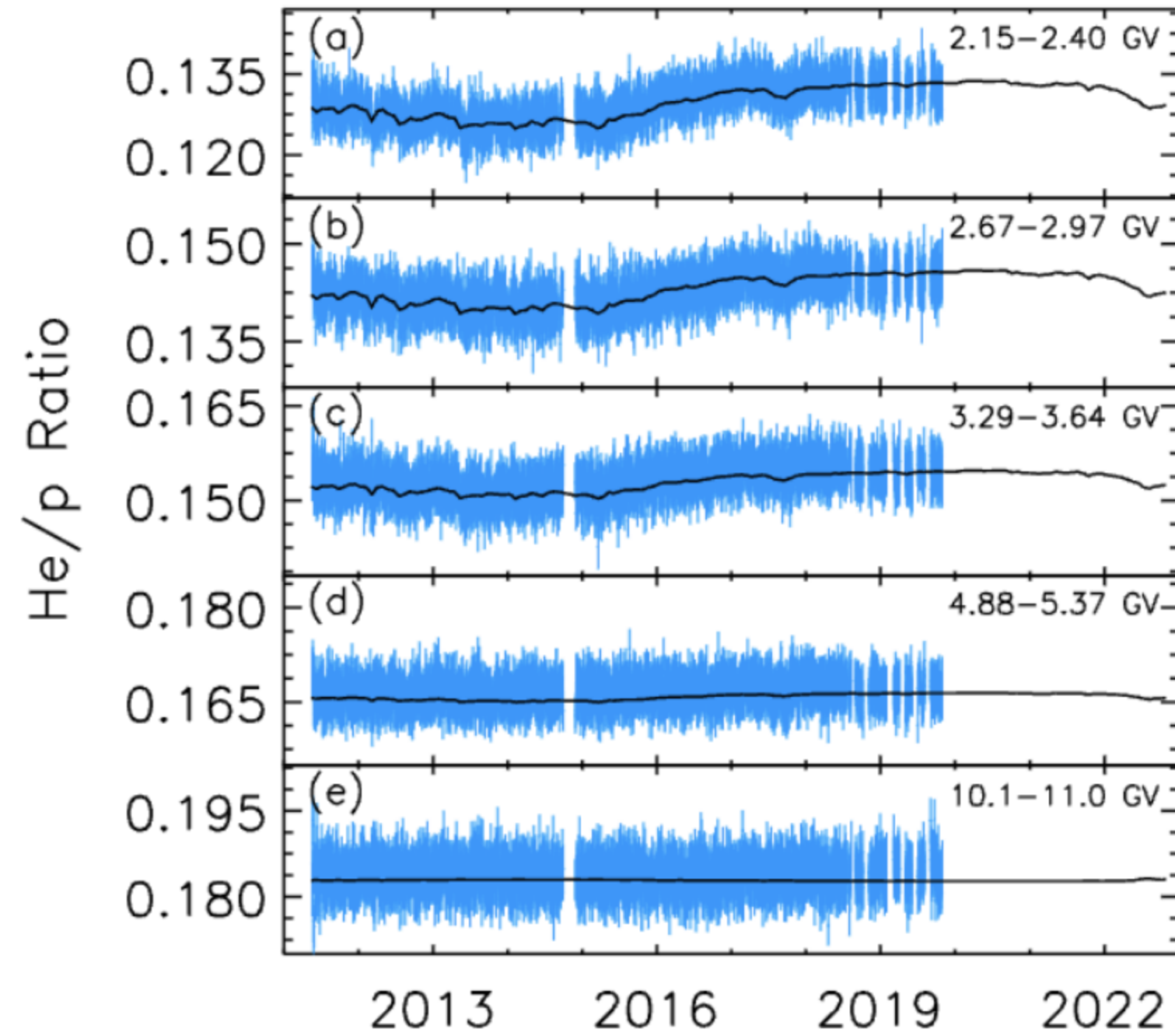
Results



Fitting to PAMELA (Martucci et al. 2018) and AMS-02 proton data (Aguilar et al. 2025).

- ϕ reflects the varying strength of solar modulation throughout the solar cycle.
- γ_1 shows smaller values during $A > 0$ solar minima compared with $A < 0$ minima.
- γ_2 is systematically larger during $A < 0$ periods than during $A > 0$ periods.

Results



Instrument	Element	RD [%]	χ^2
PAMELA	H	2.03	0.10
	He	6.80	6.39
AMS-02	H	0.19	0.042
	He	0.52	0.28
CSES-01	H	7.92	0.36

Note. The averages are computed over the periods corresponding to PAMELA (2006–2014), AMS-02 (2011–2022), and CSES-01 (2018–2022).

Using the same set of parameters derived from proton flux data, the model also successfully reproduces the solar-cycle variation of the helium flux, as well as the temporal evolution of the He/p ratio.

The dashed curves, setting the He LIS equal to the H LIS at the same rigidity.

- Distinct solar-cycle dependence of the p/He ratio at rigidities below and above ~ 0.9 GV
- Low rigidities, temporal and rigidity dependence is largely controlled by the mass-to-charge ratio.
- High rigidities (>10 GV) is mainly determined by differences in their LIS spectral shapes.

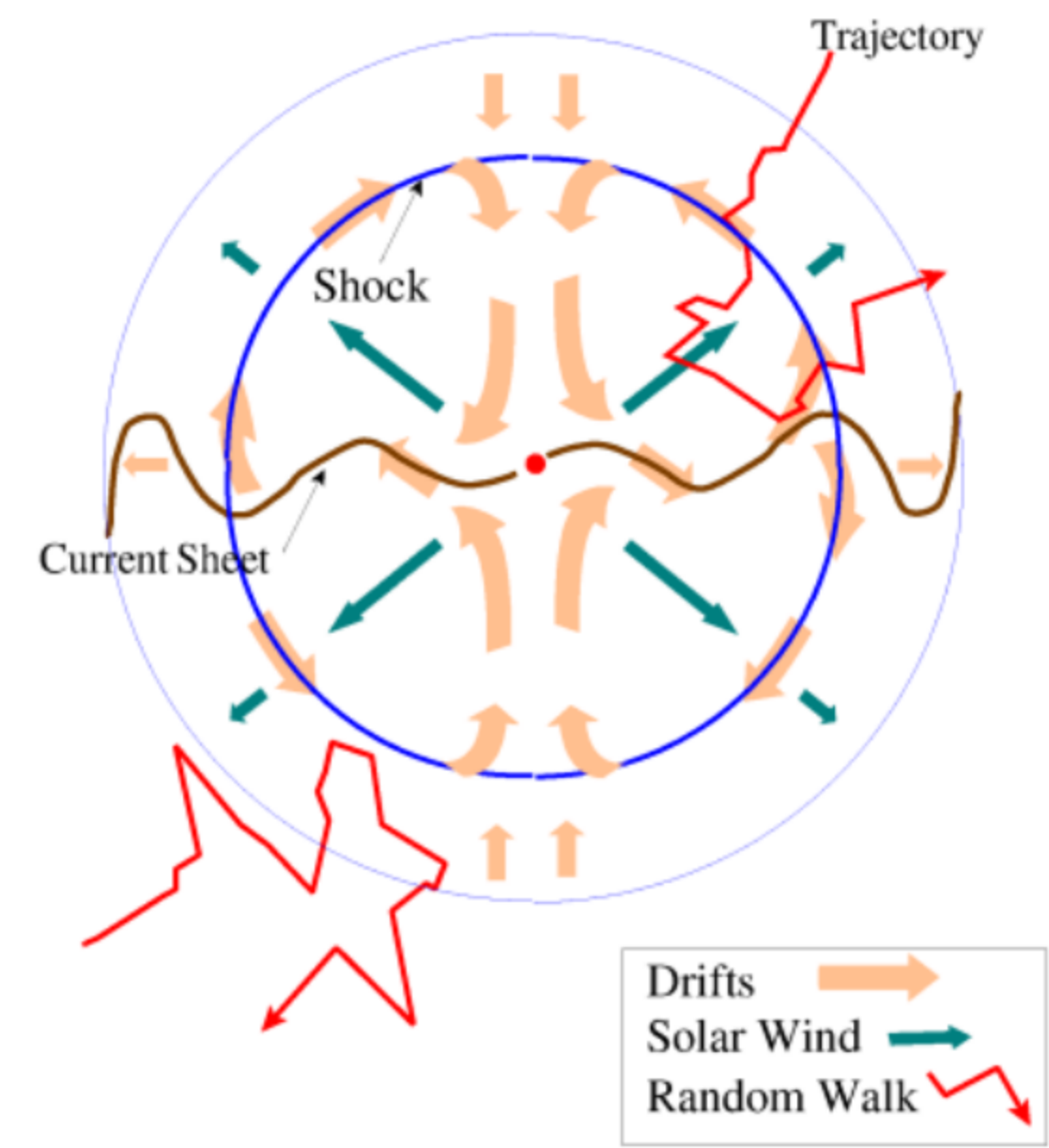
Outline

- Introduction
- The Generalized Force-field Approximation
- Result
- Discussion
- Conclusion

Discussions

The rigidity dependence of $\kappa_2(P)$:

The combined effects of **diffusion, drift, convection, and adiabatic cooling**, **trajectory-integrated** measure of particle transport from the modulation **boundary to the observer**.



Zhang & McDonald (2001), stochastic differential equations lead to

$$\langle \Delta P \rangle = \frac{2V_{sw}P}{3r \left[\frac{2\kappa_{rr}}{r} + \frac{\partial \kappa_{rr}}{\partial r} - V_{dr} - V \right]} \Delta r$$

Similar to the force-field solution, define a local diagnostic quantity

$$\kappa_2^*(r, P) = \frac{r}{2\beta} \left(\frac{2\kappa_{rr}}{r} + \frac{\partial \kappa_{rr}}{\partial r} - V_{dr} - V \right)$$

$$\mathbf{V}_d = f_s q \frac{P\beta}{3} \nabla \times \left(\frac{\mathbf{B}}{B^2} \right), \quad f_s = \frac{(P/P_A)^2}{1 + (P/P_A)^2}$$

$$\kappa_{\parallel} = \kappa_{\parallel}^0 \beta \frac{B_0}{B} \left(\frac{P}{P_0} \right)^a \left[1 + \left(\frac{P}{P_k} \right)^c \right]^{\frac{b-a}{c}}, \quad \kappa_{\perp} = 0.02 \kappa_{\parallel}$$

We set $\kappa_{\parallel}^0 = 3 \times 10^{22} \text{ cm}^2 \text{ s}^{-1}$, $a = 1.0$, and $b = 2.0$

$$dx_i = \mu_i(x_i, s)ds + \sum_{j=1}^n \sigma_{ij}(x_i, s) \cdot dW_j(s),$$

$$\mu_r = \frac{1}{r^2} \frac{\partial}{\partial r} (r^2 \kappa_{rr}) + \frac{1}{r \sin \theta} \frac{\partial}{\partial \theta} (\kappa_{\theta r} \sin \theta) + \frac{1}{r \sin \theta} \frac{\partial \kappa_{\phi r}}{\partial \phi} - V_r$$

$$\mu_{\theta} = \frac{1}{r^2} \frac{\partial}{\partial r} (r \kappa_{r\theta}) + \frac{1}{r^2 \sin \theta} \frac{\partial}{\partial \theta} (\kappa_{\theta\theta} \sin \theta) + \frac{1}{r^2 \sin \theta} \frac{\partial \kappa_{\phi\theta}}{\partial \phi} - \frac{1}{r} V_{\theta}$$

$$\mu_{\phi} = \frac{1}{r^2 \sin \theta} \frac{\partial}{\partial r} (r \kappa_{r\phi}) + \frac{1}{r^2 \sin \theta} \frac{\partial \kappa_{\theta\phi}}{\partial \theta} + \frac{1}{r^2 \sin^2 \theta} \frac{\partial \kappa_{\phi\phi}}{\partial \phi} - \frac{1}{r \sin \theta} V_{\phi}$$

$$\mu_p = \frac{p}{3} (\nabla \cdot \vec{V}_{sw}),$$

Discussions

The generalized force field approximation:

$$J(E) = J_{\text{LIS}}(E_b) \frac{E(E + 2E_0)}{E_b(E_b + 2E_0)}$$

$$\phi = \frac{A}{Z} \int_E^{E_b} \frac{\kappa_2(P)}{P} dE'$$

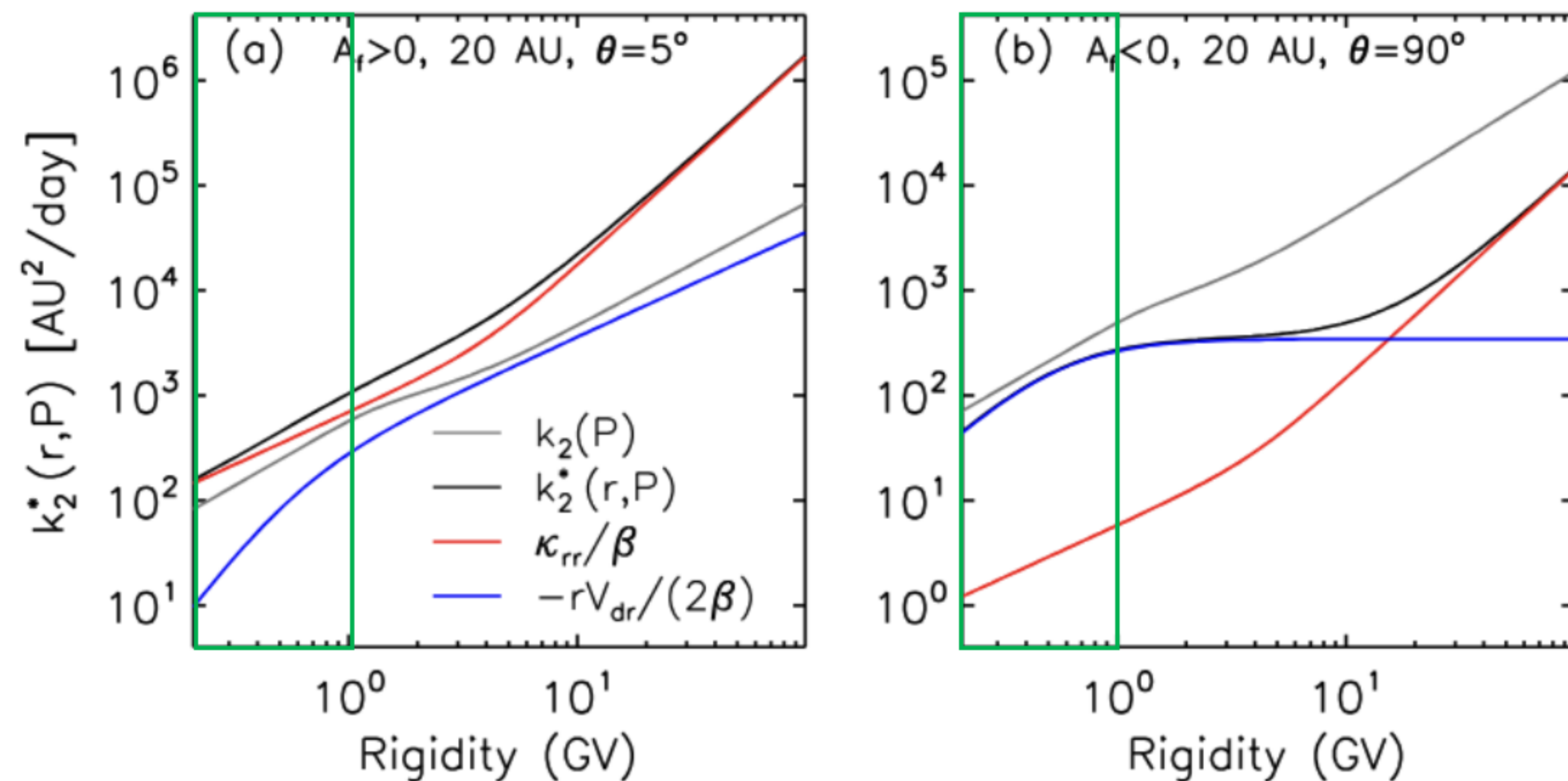
$$\kappa_2(P) = P_0 \left(\frac{P}{P_0} \right)^{\gamma_0} \left(1 + \left(\frac{P}{P_{k1}} \right)^{s_1} \right)^{\frac{\gamma_1 - \gamma_0}{s_1}} \left(1 + \left(\frac{P}{P_{k2}} \right)^{s_2} \right)^{\frac{\gamma_2 - \gamma_1}{s_2}}$$

Below $\sim 1\text{GV}$, the spectral index of $\kappa_2(P)$ $\gamma_0 = 1.25$

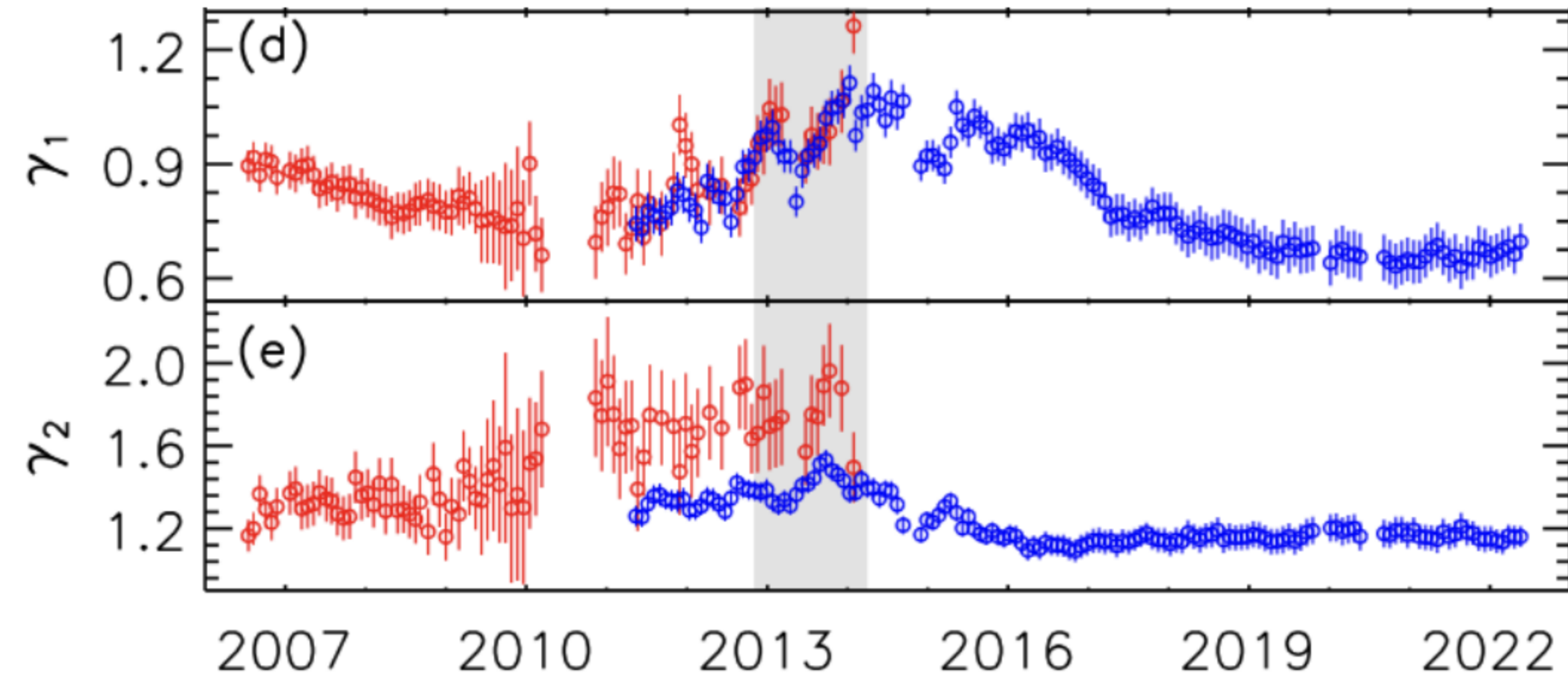
➤ $A_f > 0$ epochs, Drift term is small relative to diffusion, but the the extended polar residence, combined with convection, steepens the rigidity dependence.

➤ $A_f < 0$ epochs, the local drift can exceed diffusion near the HCS. But limited to $\sim 2R_L$, declines rapidly away from the HCS.

Drift contribution to $\kappa_2(P)$ is smaller than that implied by the local behaviour of $\kappa_2^*(r, P)$

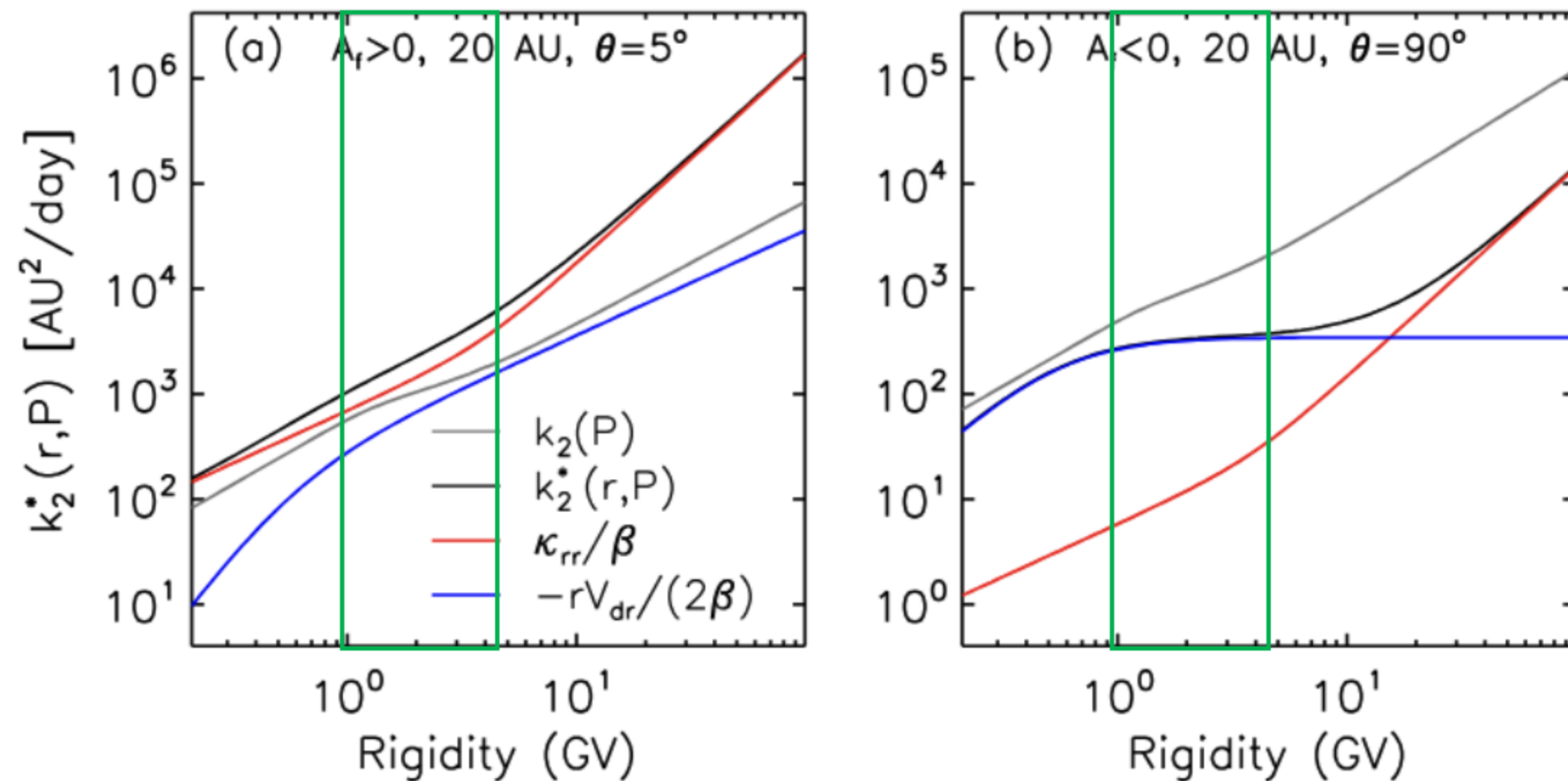


Discussions



In the range $P \sim 1 - 4\text{GV}$, $0 < \gamma_1 < 1$.

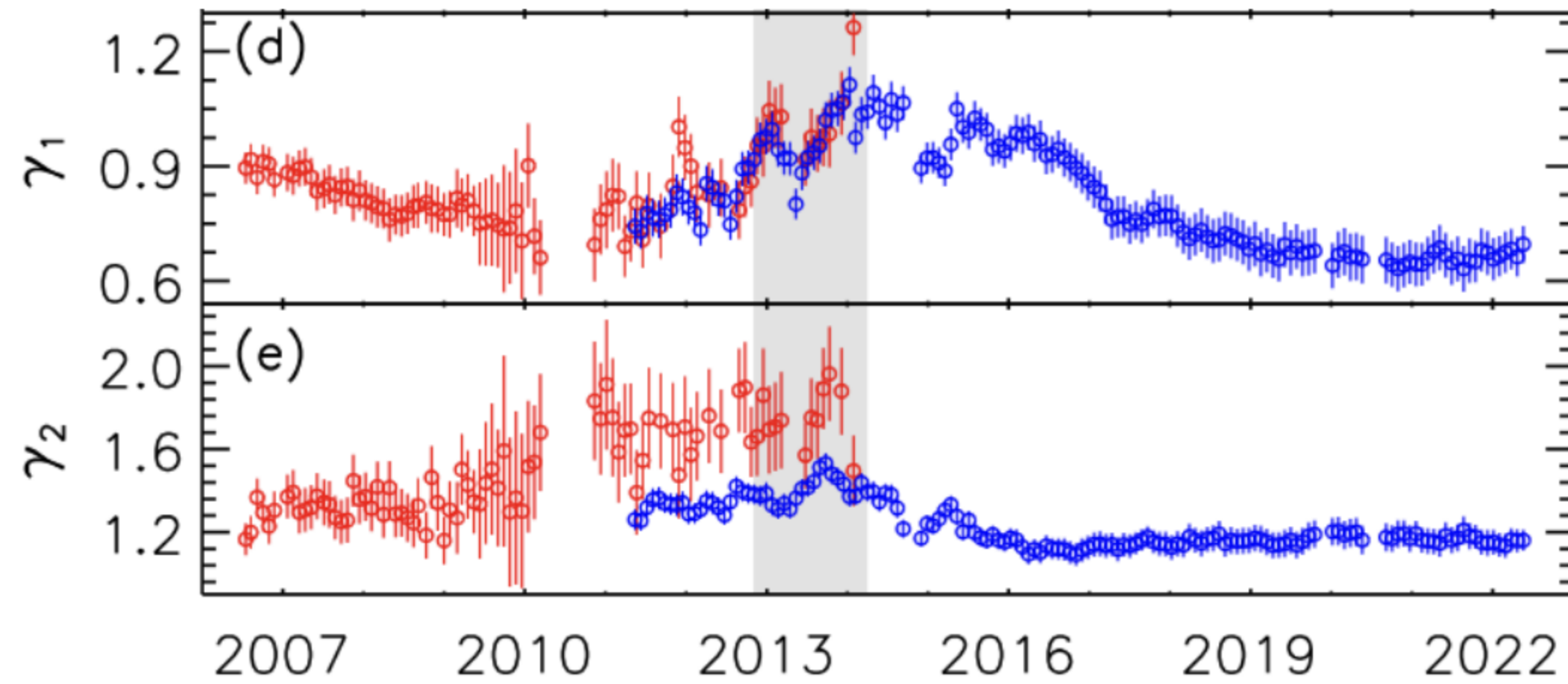
- $A_f > 0$ epochs, at high latitudes, the diffusion and drift contributions to $\kappa_2^*(r, P)$ are comparable in magnitude, resulting in $0 < \gamma_1 < 1$.
- $A_f < 0$ epochs, As rigidity increases, the influence of the HCS declines, enhancing the contrast between low and high rigidities and yielding larger γ_1 values than in the $A_f > 0$ case.



Numerical simulations (e.g. Corti et al. 2019; X. Song et al. 2025) indicate that the spectral index of the diffusion coefficient below $\sim 4\text{GV}$ shows little variation over the solar cycle. Particle drifts exhibit a pronounced solar cycle dependence.

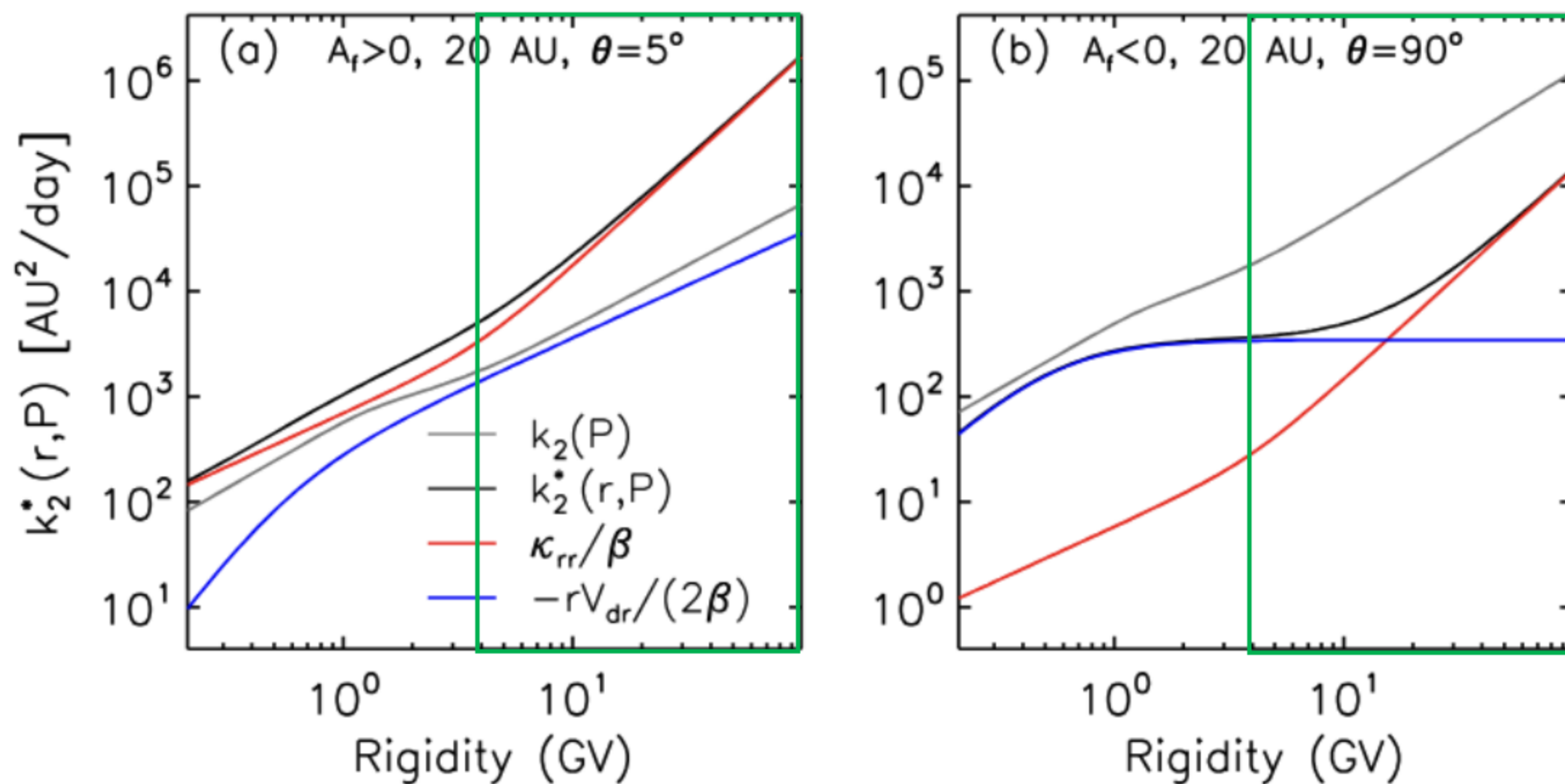
Larger γ_1 during solar maximum implies a reduced contribution from drift, smaller γ_1 during solar minimum indicates an enhanced drift contribution.

Discussions



At rigidities $P \gtrsim 4\text{GV}$, the rigidity dependence of $\kappa_2(P)$ is largely diffusion controlled.

- $A_f > 0$ epochs, the extended polar residence enhances the cumulative effect of drift along particle trajectories, resulting in systematically smaller values of γ_2 compared with those during $A_f < 0$ epochs.
- $A_f < 0$ epochs, particles spend an increasingly small fraction of their trajectories in the vicinity of the HCS, γ_2 is primarily determined by diffusion, with only a negligible contribution from drift effects.



The global, trajectory-integrated quantity $\kappa_2(P)$ cannot be inferred directly from local diffusion and drift coefficients

Diffusion coefficients derived from force-field fits, cannot be mapped into the local coefficients used in transport theory or implemented in numerical simulations

Outline

- Introduction
- The Generalized Force-field Approximation
- Result
- Discussion
- Conclusion

Conclusions



We present a generalized FFA model in this work.

The rigidity dependence of $\kappa_2(P)$ is mainly governed by diffusion, with drift effects producing a noticeable modification at rigidities below $\sim 4\text{GV}$ and giving rise to a triple power-law form for $\kappa_2(P)$.

The model captures the essential rigidity and A/Z dependencies, achieves higher computational efficiency while maintaining an accuracy in reproducing cosmic ray flux measurements.

Our results can be readily extended to other elements, such as boron and carbon, and are expected to provide useful insights into the rigidity dependence of secondary-to-primary ratios.

Thank you!

Backup

